Peatlands and their carbon dynamics in northern high latitudes from 1990 to 2300: A process-based biogeochemistry model analysis

Bailu Zhao[1], Qianlai Zhuang[1, 2]

[1] Department of Earth, Atmospheric, and Planetary Sciences, Purdue University, West Lafayette, IN 47907, USA

[2] Department of Agronomy, Purdue University, West Lafayette, IN 47907, USA

Correspondence to: Qianlai Zhuang (qzhuang@purdue.edu)

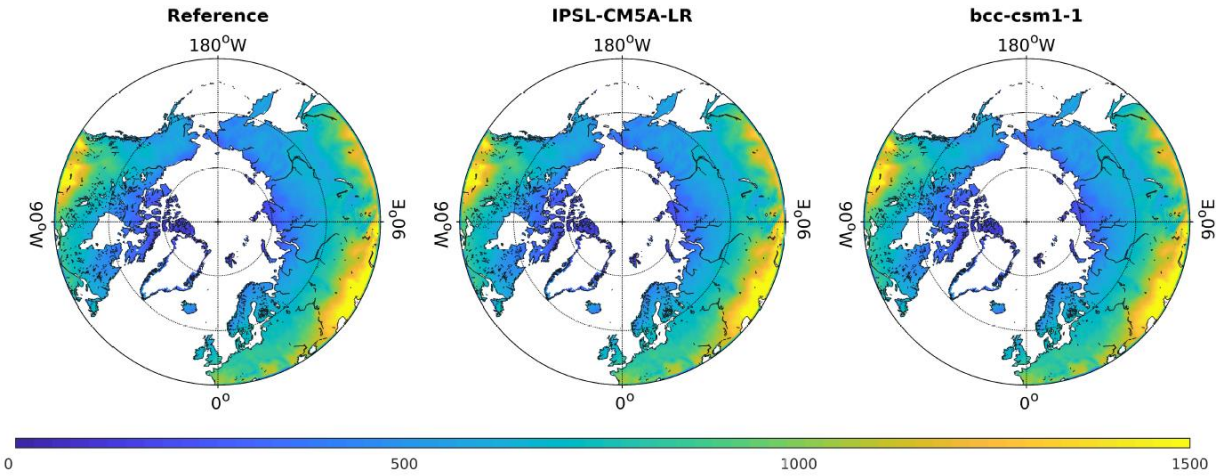

Figure S1. Comparison between the reference and calibrated annual PET (mm). The reference dataset is the global aridity index and potential evapotranspiration (ET0) database v3 (Zomer and Trabucco, 2022), and calibration is conducted for IPSL-CM5A-LR and bcc-csm1-1 climate inputs, respectively.

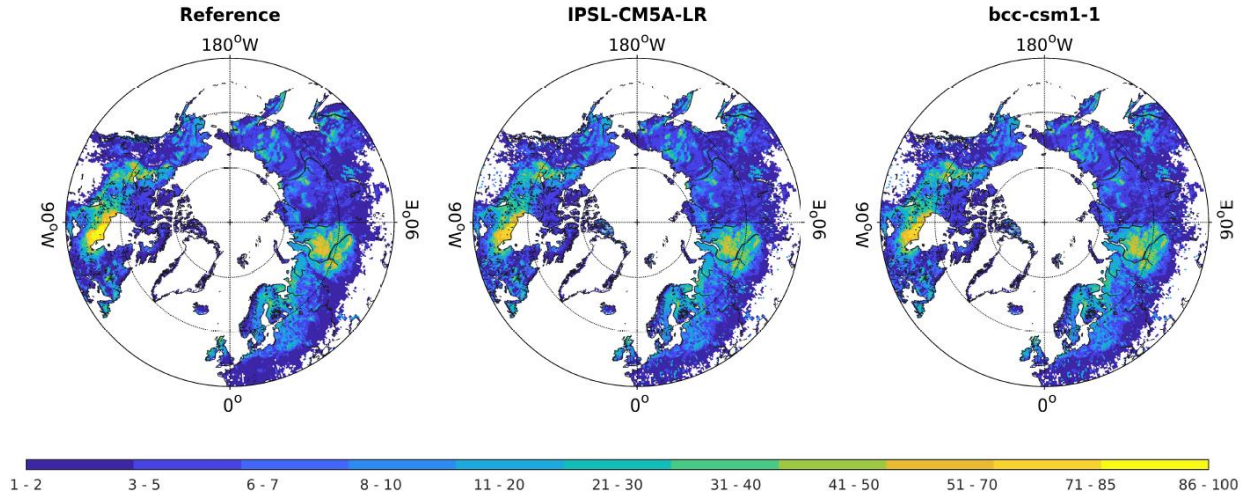

Figure S2. Comparison between the reference and calibrated wetland abundance (%) interpolated with TOPMODEL approach. The reference dataset is the average peatland abundance of three peatland maps (Xu et al., 2018; Hugelius et al., 2020; Melton et al., 2022), and calibration is conducted for IPSL-CM5A-LR and bcc-csm1-1 climate inputs, respectively. The grid cells with less than 1% wetlands are left blank.

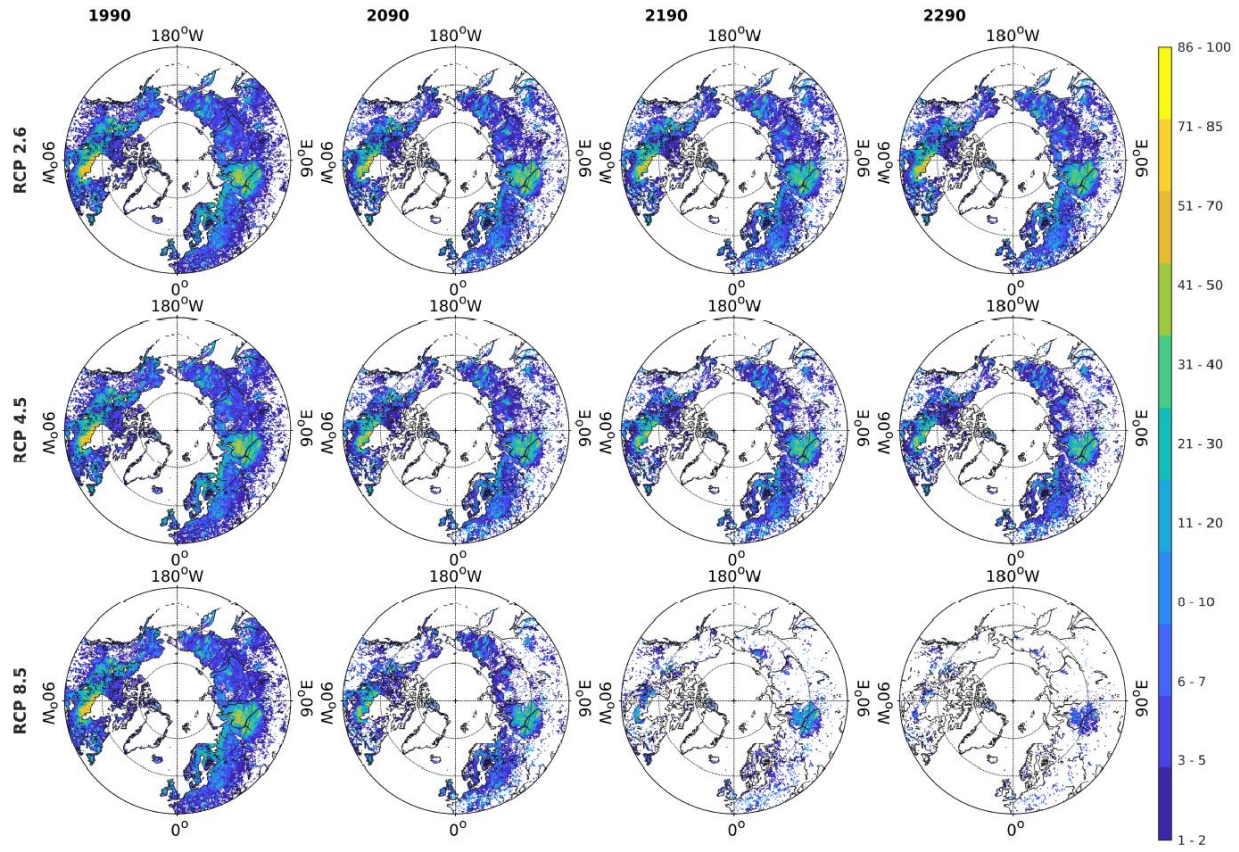

Figure S3. Distribution of wetlands abundance (%) with IPSL-CM5A-LR input forcing under RCP 2.6, RCP 4.5 and RCP 8.5. The grid cells with less than 1% wetlands are left blank.

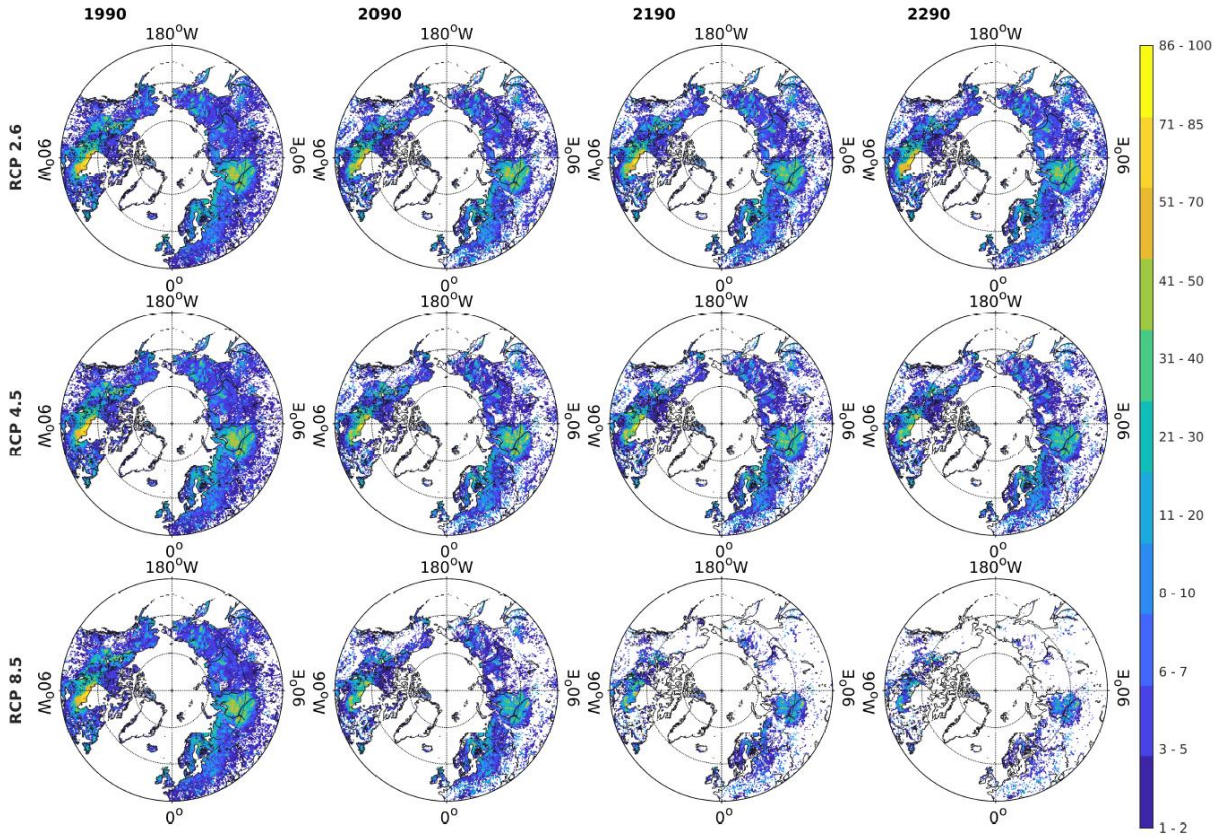

Figure S4. Distribution of wetlands abundance (%) with bcc-csm1-1 input forcing under RCP 2.6, RCP 4.5 and RCP 8.5. The grid cells with less than 1% wetlands are left blank.

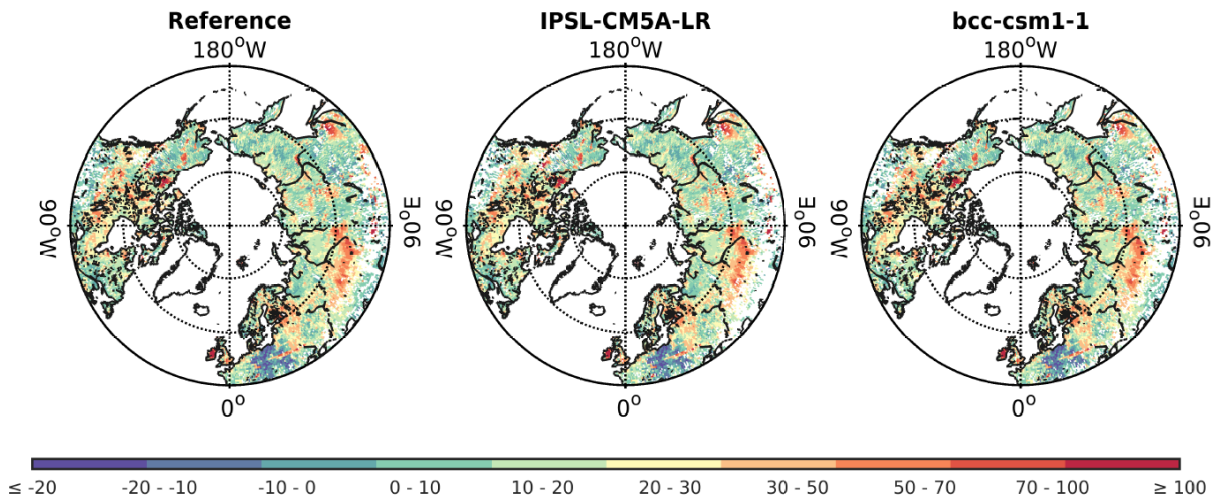

Figure S5. Comparison between the 50-year (1940-1990) reference (Zhao et al., 2022) and calibrated C accumulation rate ($gC \cdot m^{-2} \cdot yr^{-1}$).

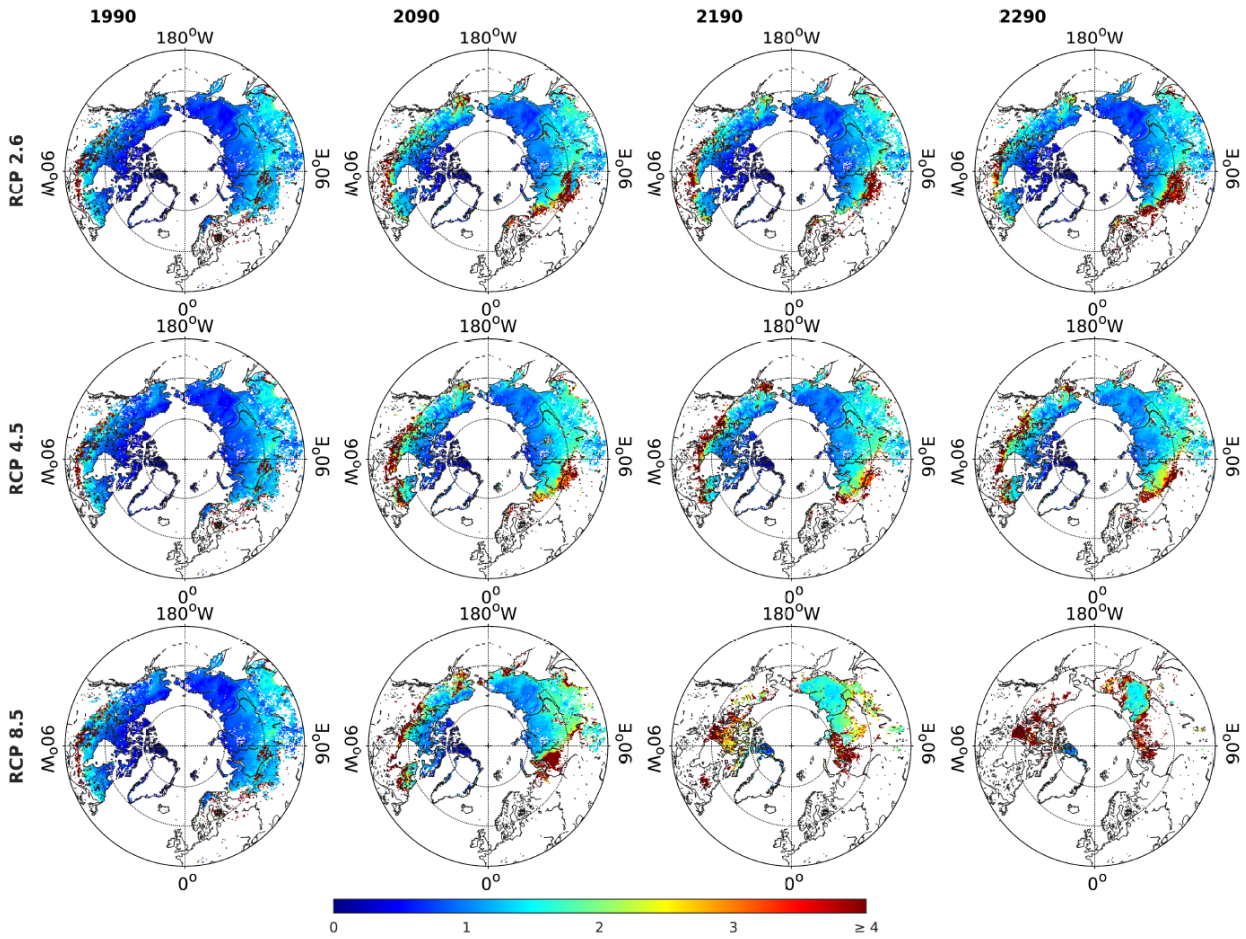

Figure S6. Active layer depth (m) with IPSL-CM5A-LR forcing input in 1990, 2090, 2190 and 2290.

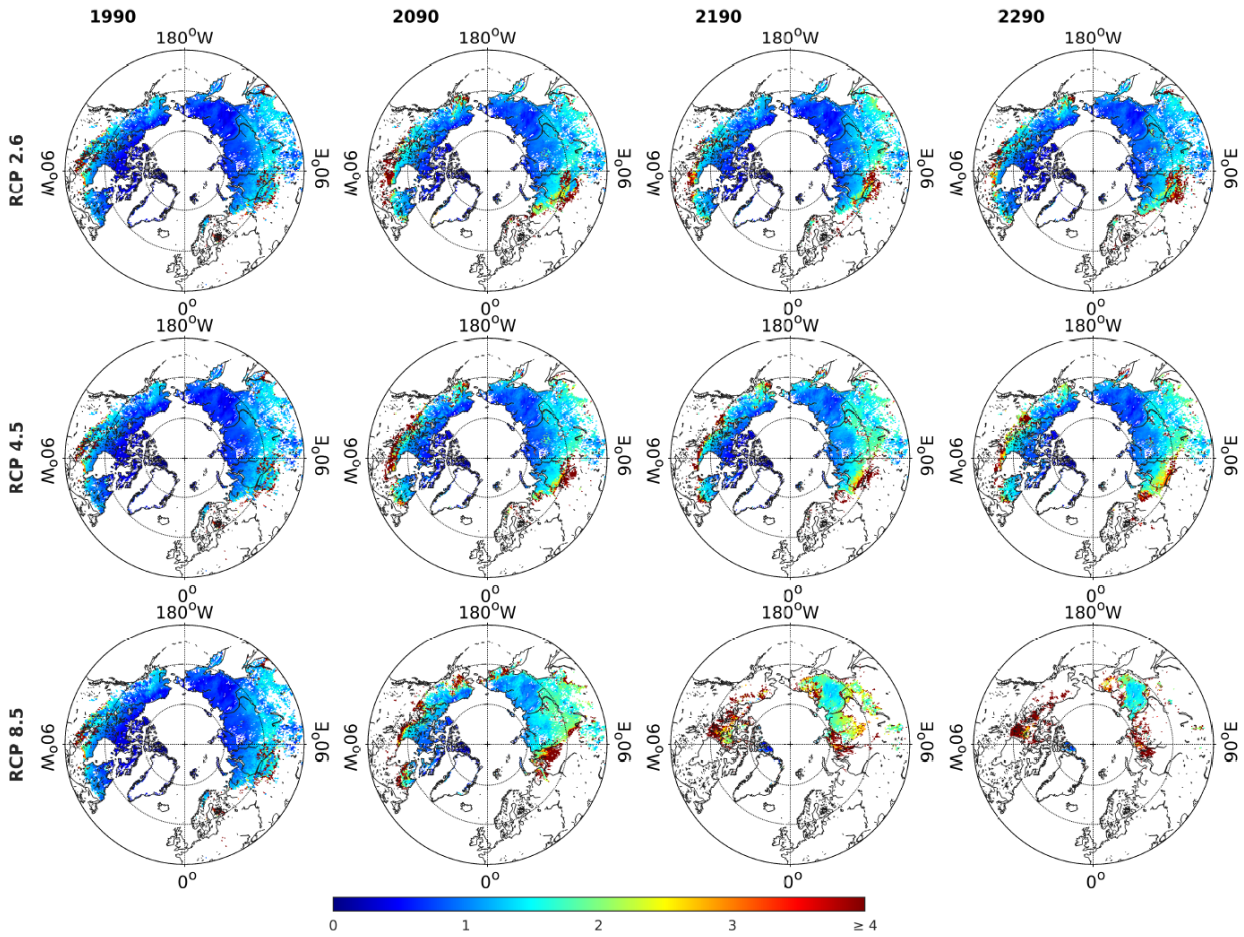

Figure S7. Active layer depth (m) with bcc-csm1-1 forcing input in 1990, 2090, 2190 and 2290.

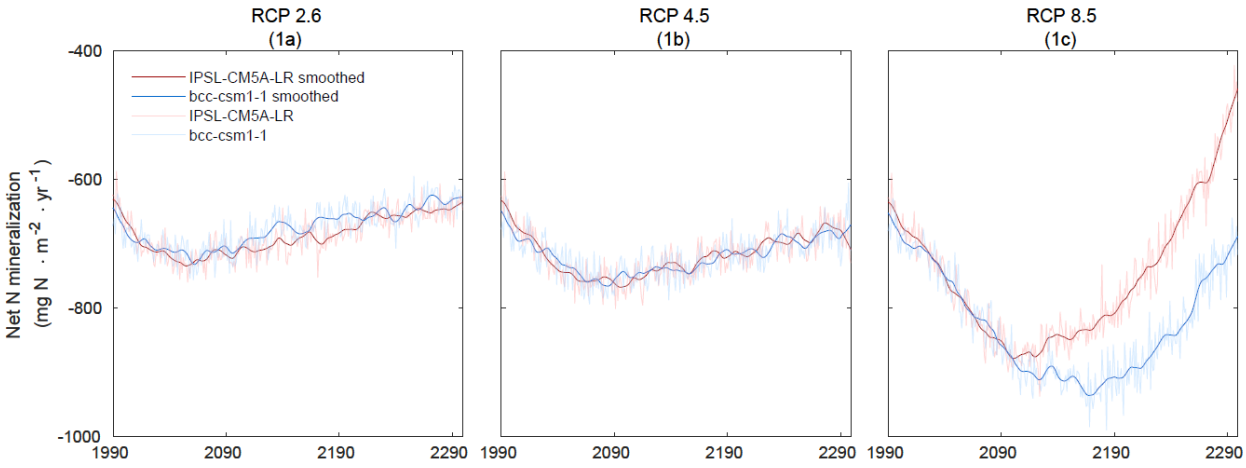

Figure S8. Time series of pan-Arctic peatland average net N mineralization rate C ($mgN \cdot m^{-2} \cdot yr^{-1}$). Lower negative values indicate more net N mineralization and more plant available N in soils.

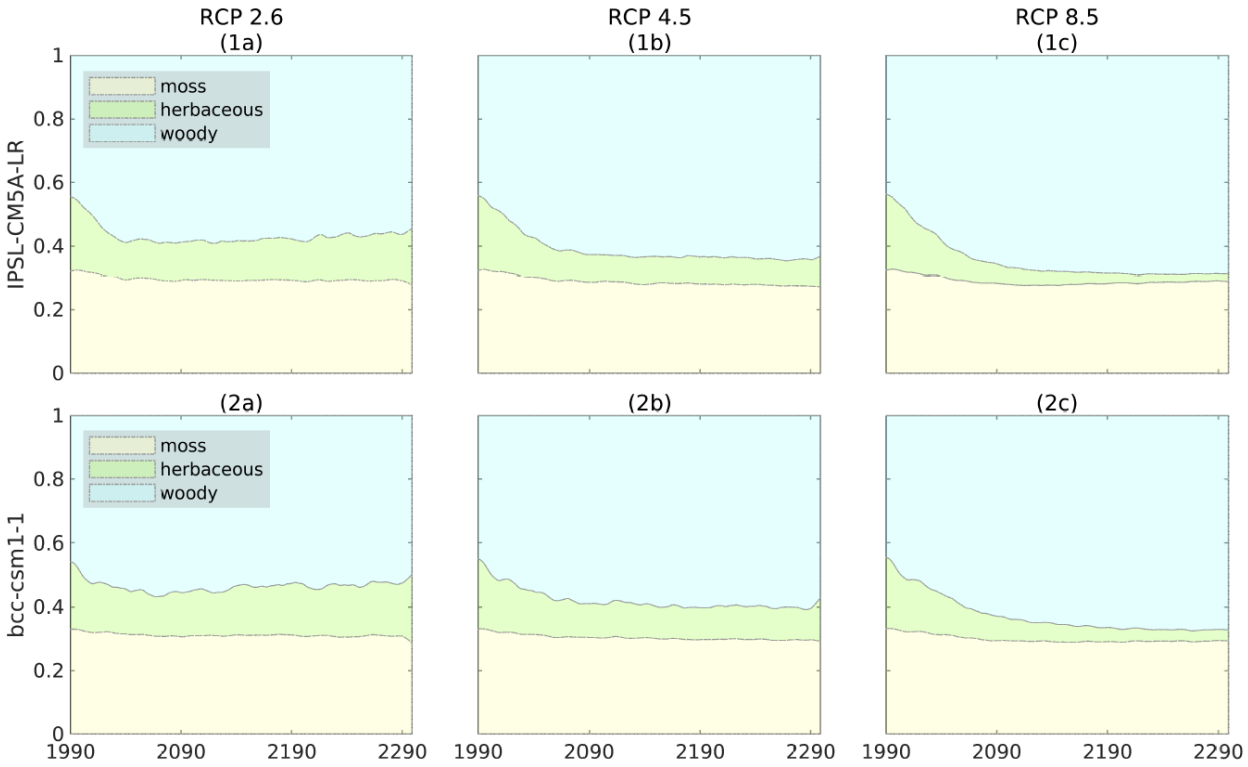

Figure S9. Time series of pan-Arctic peatland plant functional type (PFT) dominance estimated from the relative abundance of PFT vegetation C ($gC \cdot m^{-2} \cdot yr^{-1}$).

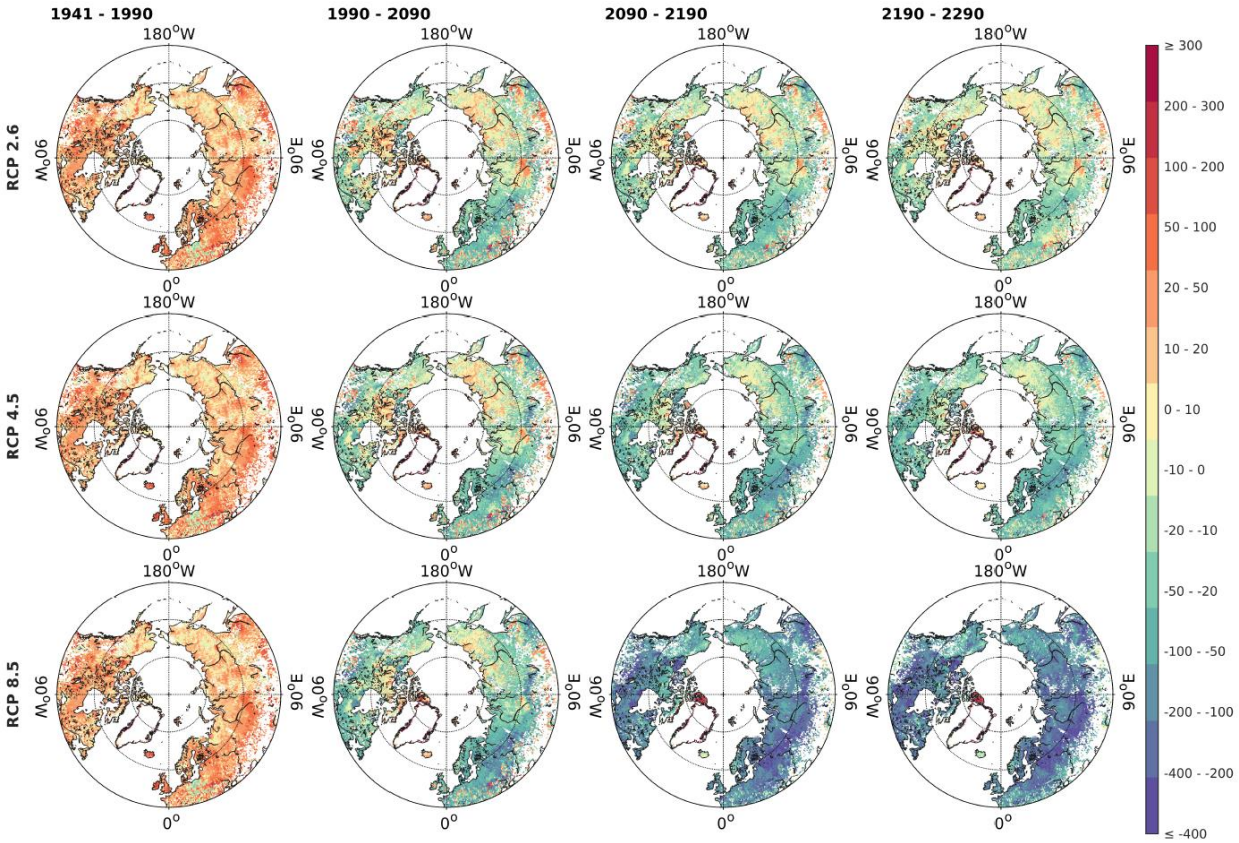

Figure S10. C accumulation rate ($gC \cdot m^{-2} \cdot yr^{-1}$) with IPSL-CM5A-LR forcing input during 1940-1990, 1990-2090, 2090-2190 and 2190-2290.

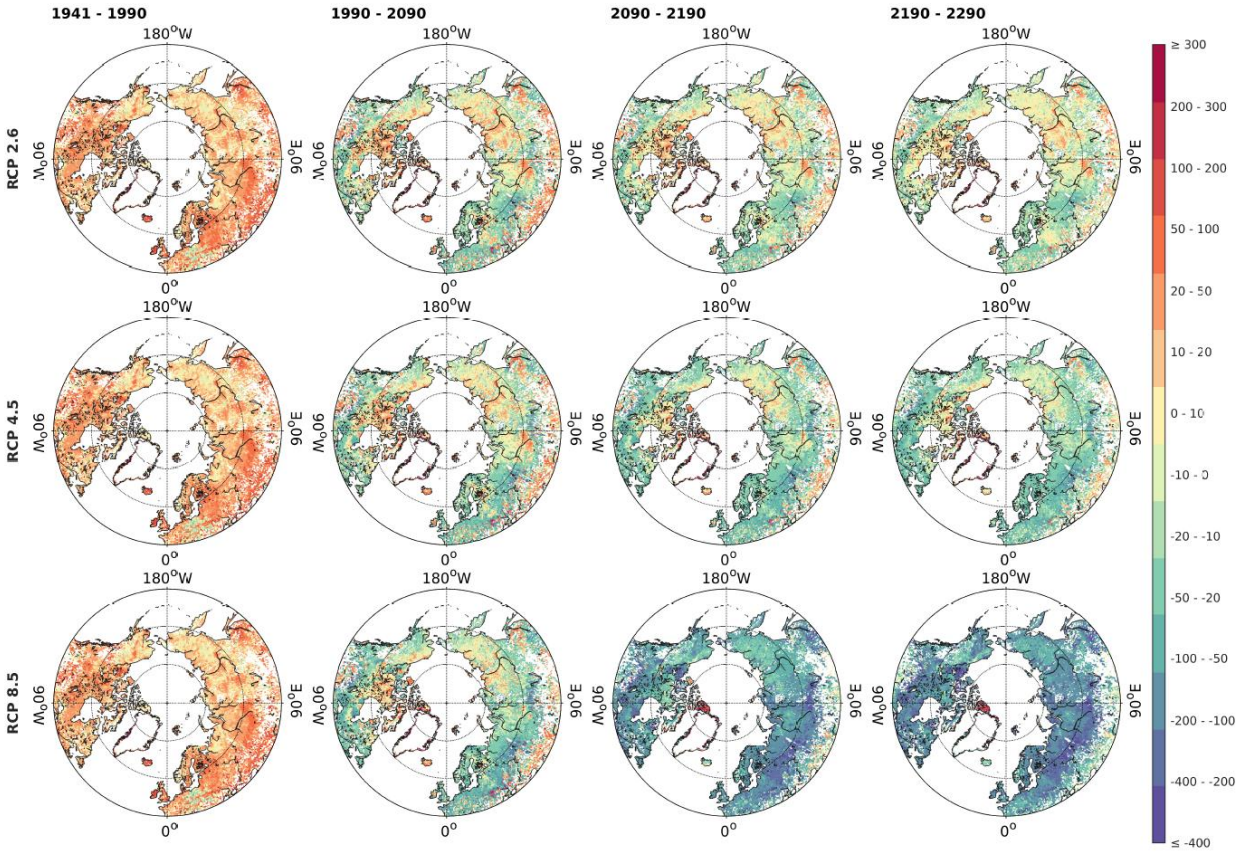

Figure S11. C accumulation rate ($gC \cdot m^{-2} \cdot yr^{-1}$) with bcc-csm1-1 forcing input during 1940-1990, 1990-2090, 2090-2190 and 2190-2290.

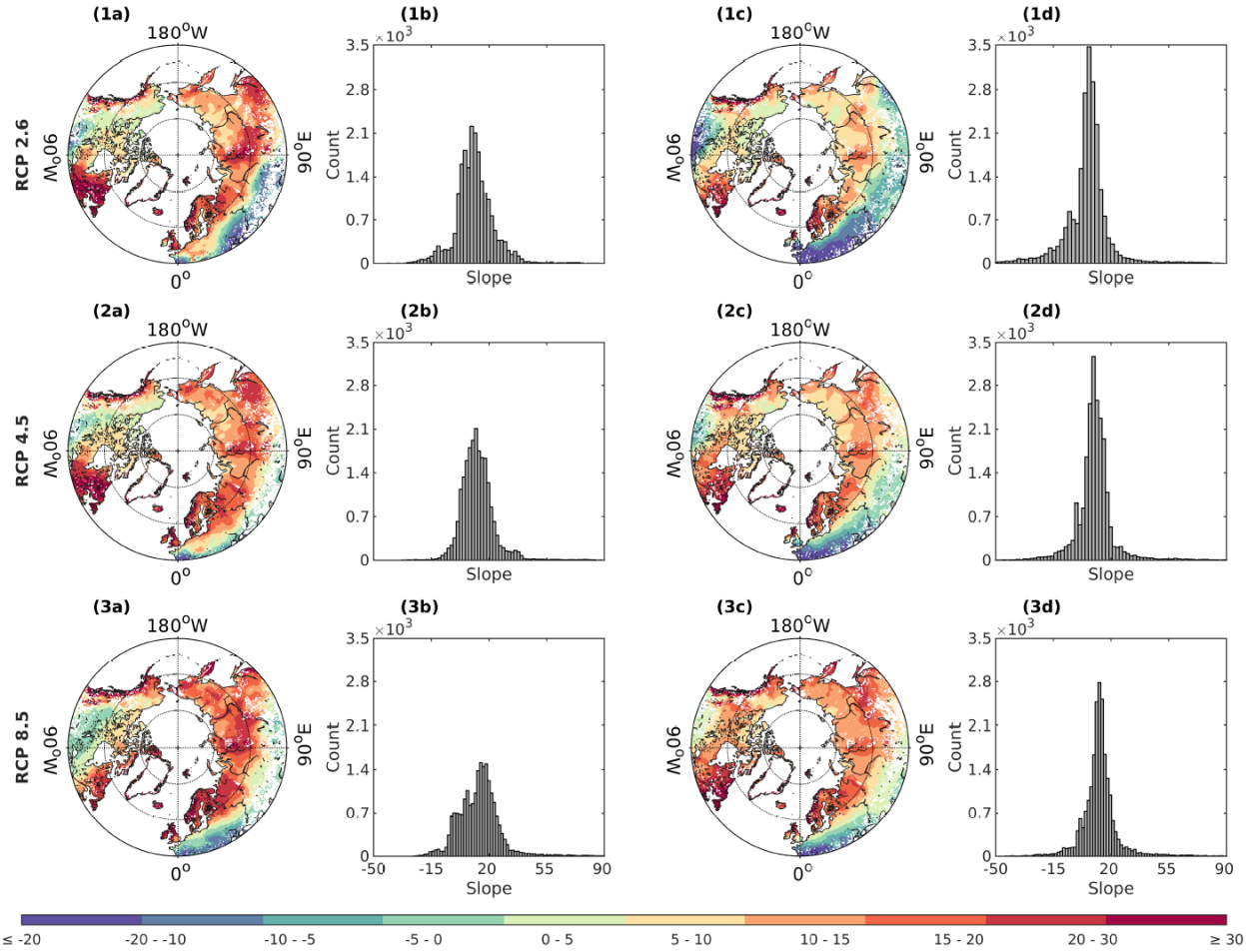

Figure S12. Correlation coefficients and their histograms between annual temperature (°C) and annual precipitation (mm) of the forcing data. Panel (a): the correlation coefficient of IPSL-CM5A-LR forcing; panel (b): the histogram of panel (a); panel (c): the correlation coefficient of bcc-csm1-1 forcing; panel (d): the histogram of panel (c).

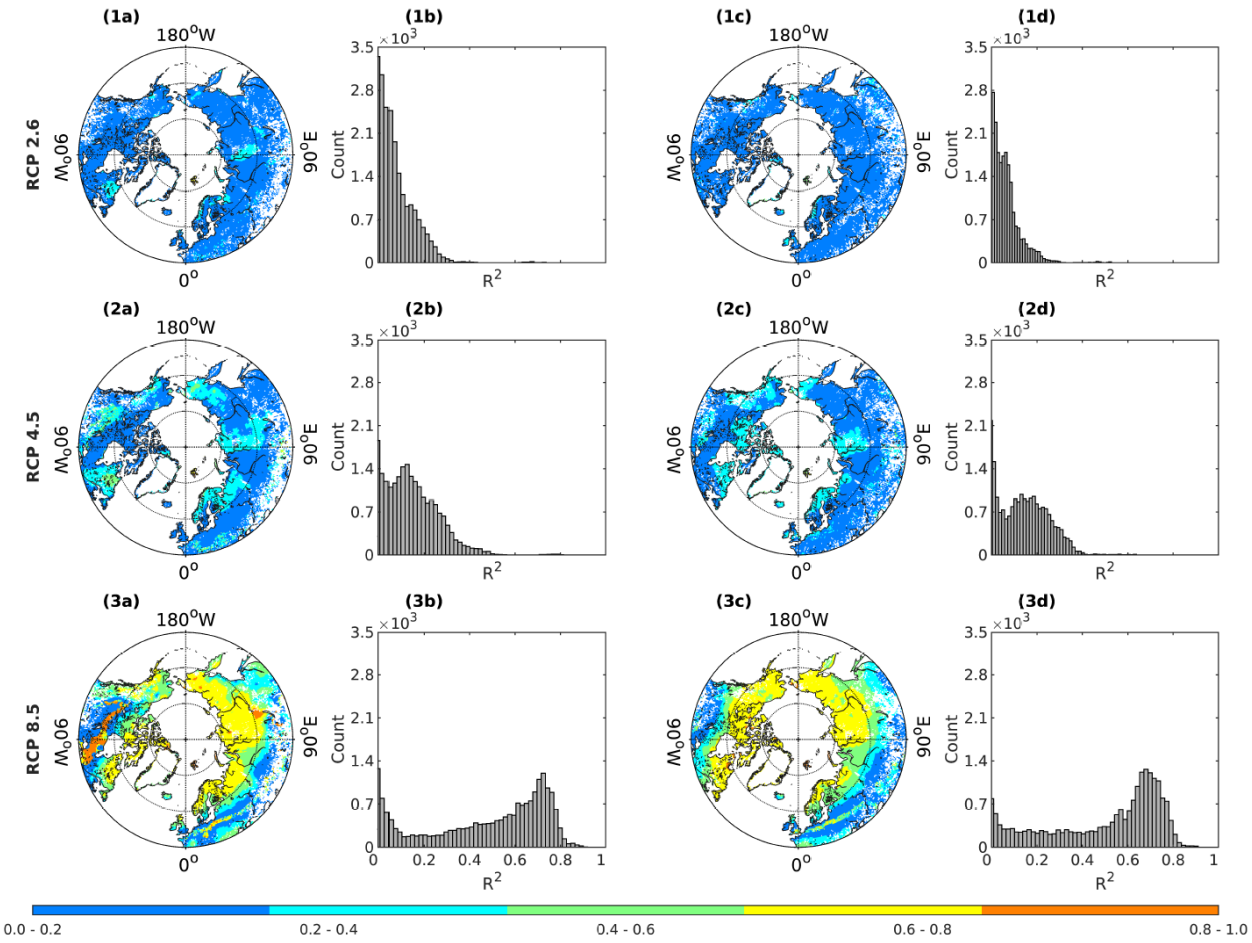

Figure S13. R^2 values and their histograms of the correlation between annual temperature (°C) and annual precipitation (mm) of the forcing data. Panel (a): the R^2 values with IPSL-CM5A-LR forcing; panel (b): the histogram of panel (a); panel (c): the R^2 values with bcc-csm1-1 forcing; panel (d): the histogram of panel (c).

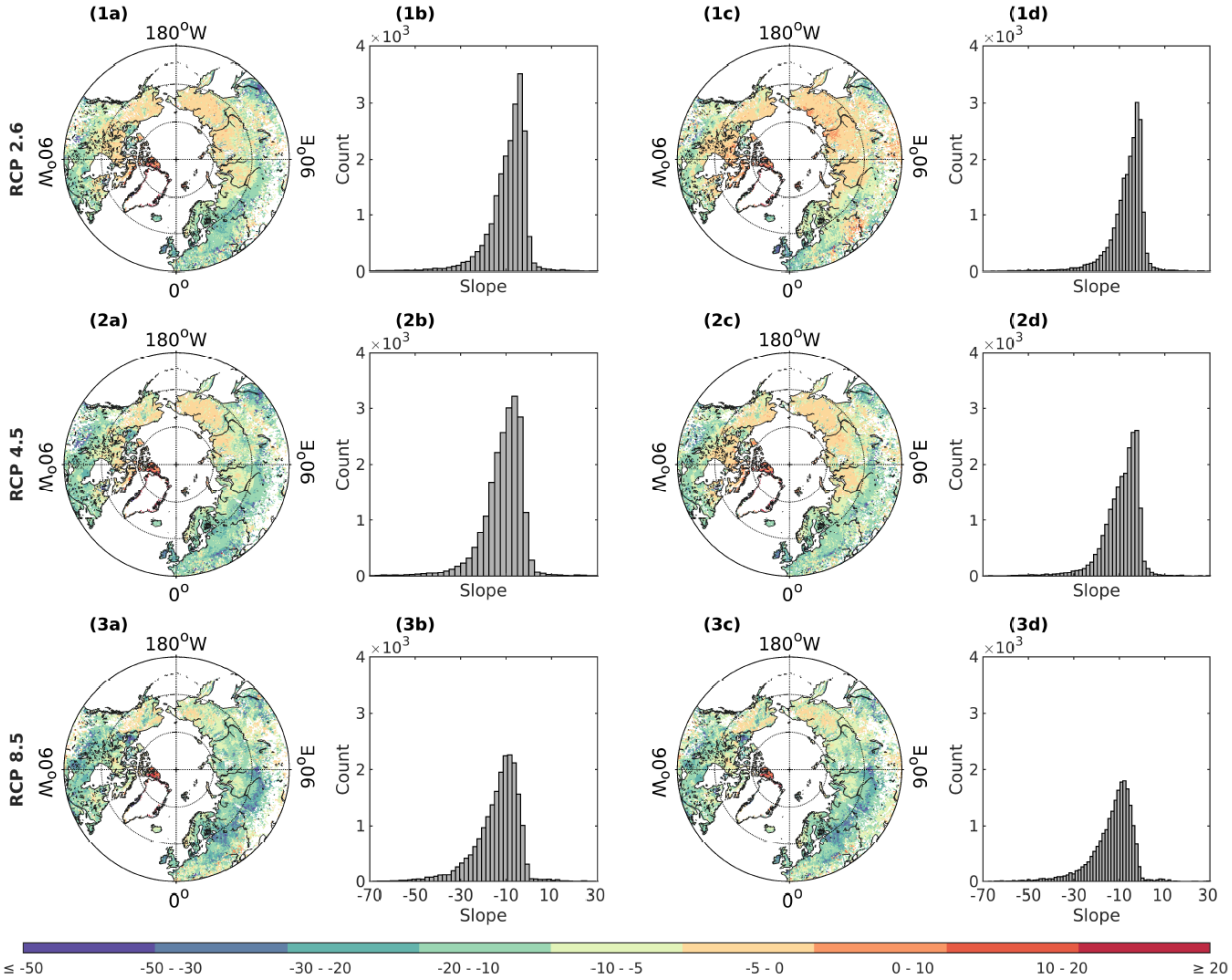

Figure S14. Correlation coefficients and their histograms between annual temperature (°C) and peatland C sink capability ($gC \cdot m^{-2} \cdot yr^{-1}$). Panel (a): the correlation coefficient of IPSL-CM5A-LR forcing; panel (b): the histogram of panel (a); panel (c): the correlation coefficient of bcc-csm1-1 forcing; panel (d): the histogram of panel (c).

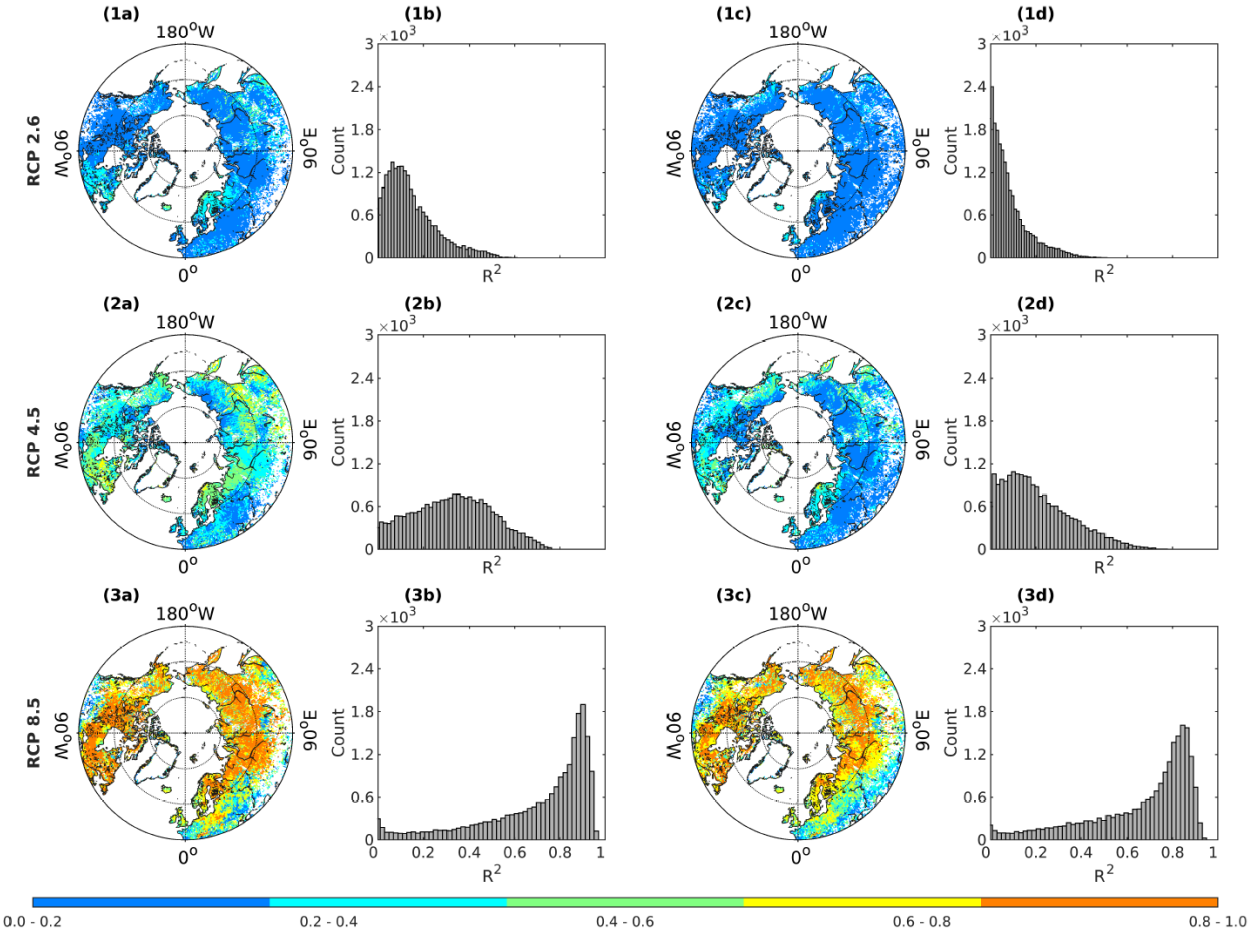

Figure S15. R^2 values and their histograms of the correlation between annual temperature (°C) and peatland C sink capability ($gC \cdot m^{-2} \cdot yr^{-1}$). Panel (a): the R^2 values with IPSL-CM5A-LR forcing; panel (b): the histogram of panel (a); panel (c): the R^2 values with bcc-csm1-1 forcing; panel (d): the histogram of panel (c).

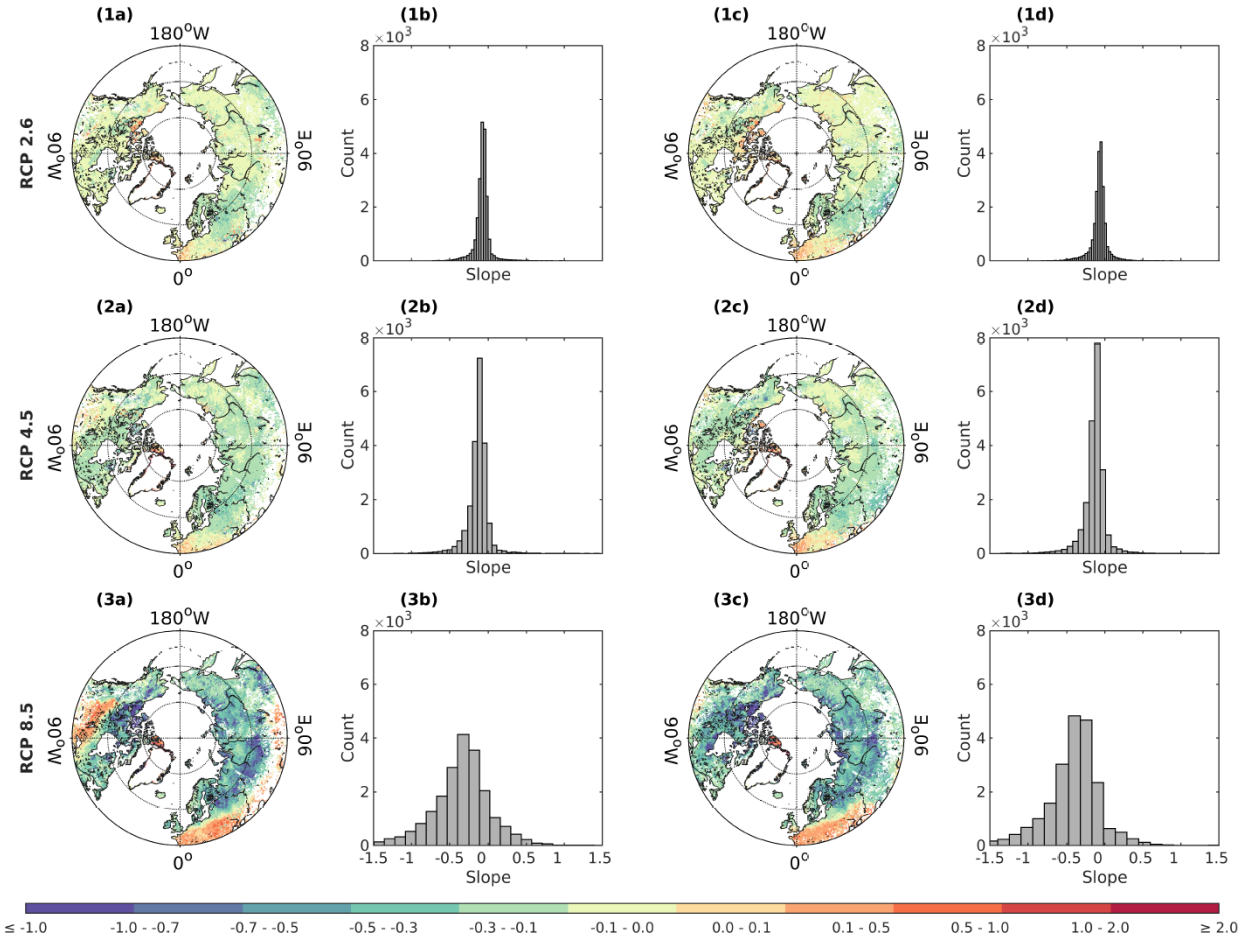

Figure S16. Correlation coefficients and their histograms between annual precipitation (mm) and peatland C sink capability ($gC \cdot m^{-2} \cdot yr^{-1}$). Panel (a): the correlation coefficient of IPSL-CM5A-LR forcing; panel (b): the histogram of panel (a); panel (c): the correlation coefficient of bcc-csm1-1 forcing; panel (d): the histogram of panel (c).

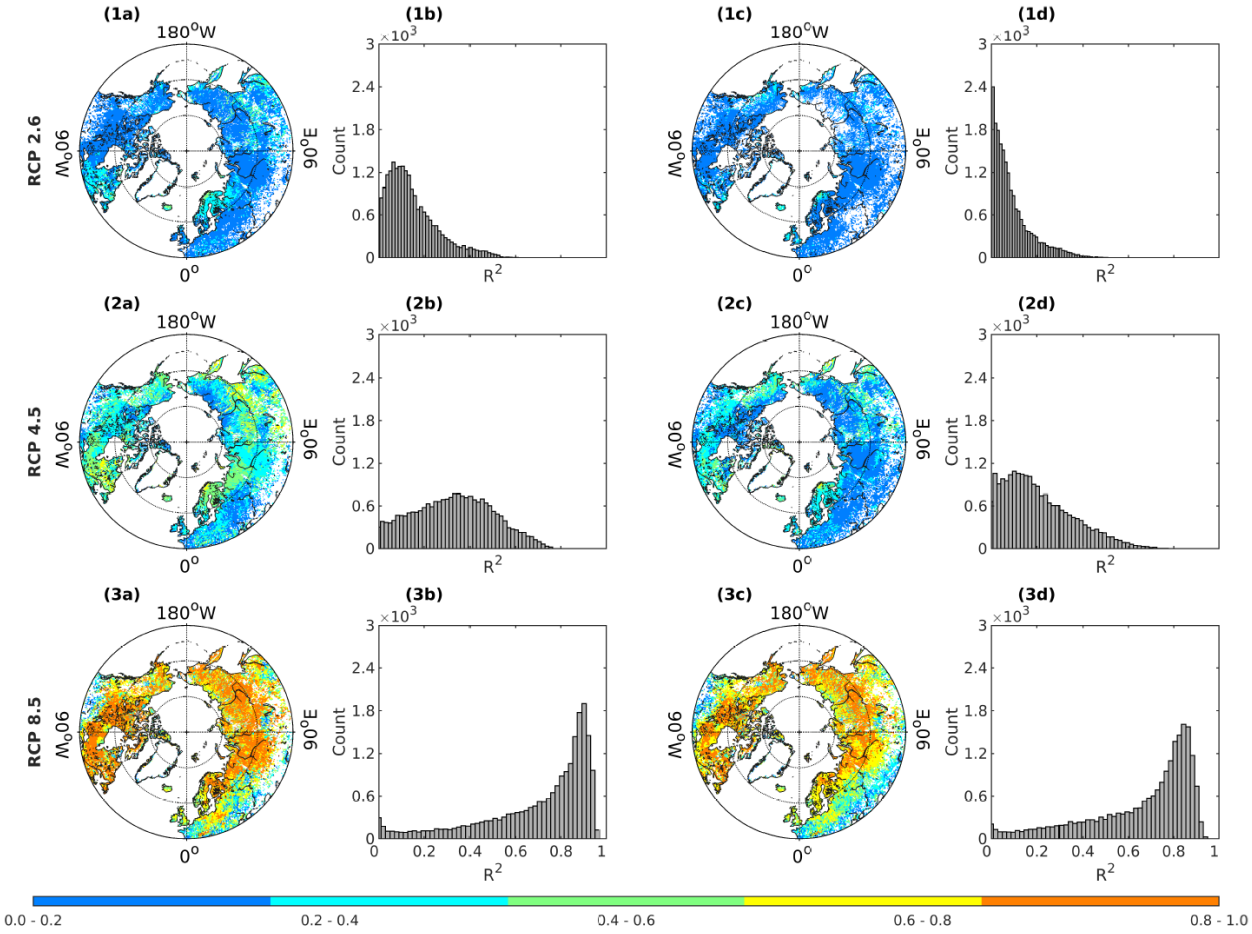

Figure S17. R^2 values and their histograms of the correlation between annual precipitation (mm) and peatland C sink capability ($gC \cdot m^{-2} \cdot yr^{-1}$). Panel (a): the R^2 values with IPSL-CM5A-LR forcing; panel (b): the histogram of panel (a); panel (c): the R^2 values with bcc-csm1-1 forcing; panel (d): the histogram of panel (c).

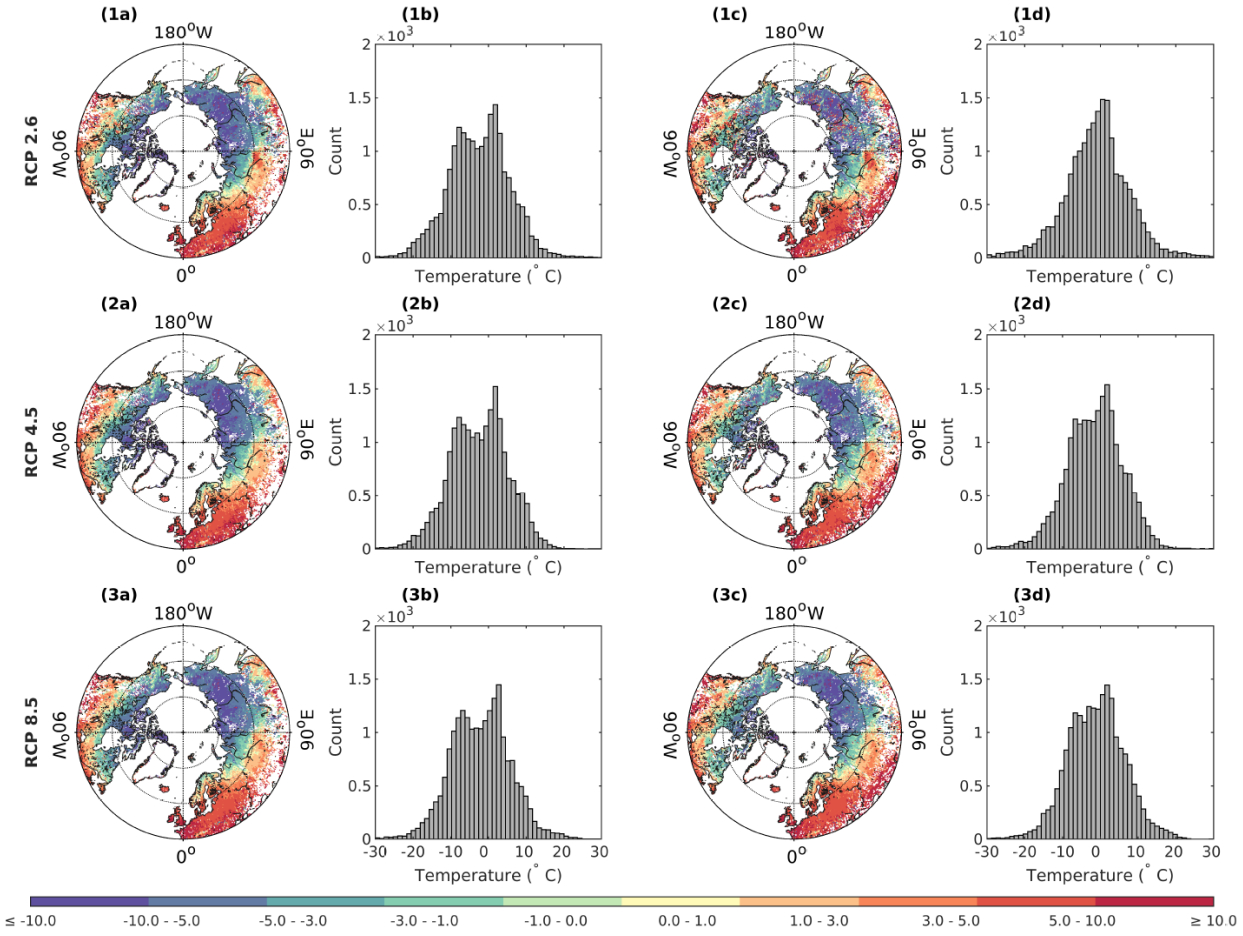

Figure S18. Threshold annual temperature (°C) of peatland C sink-source shift. Panel (a): the threshold temperature of IPSL-CM5A-LR forcing; panel (b): the histogram of panel (a); panel (c): the threshold temperature of bcc-csm1-1 forcing; panel (d): the histogram of panel (c).

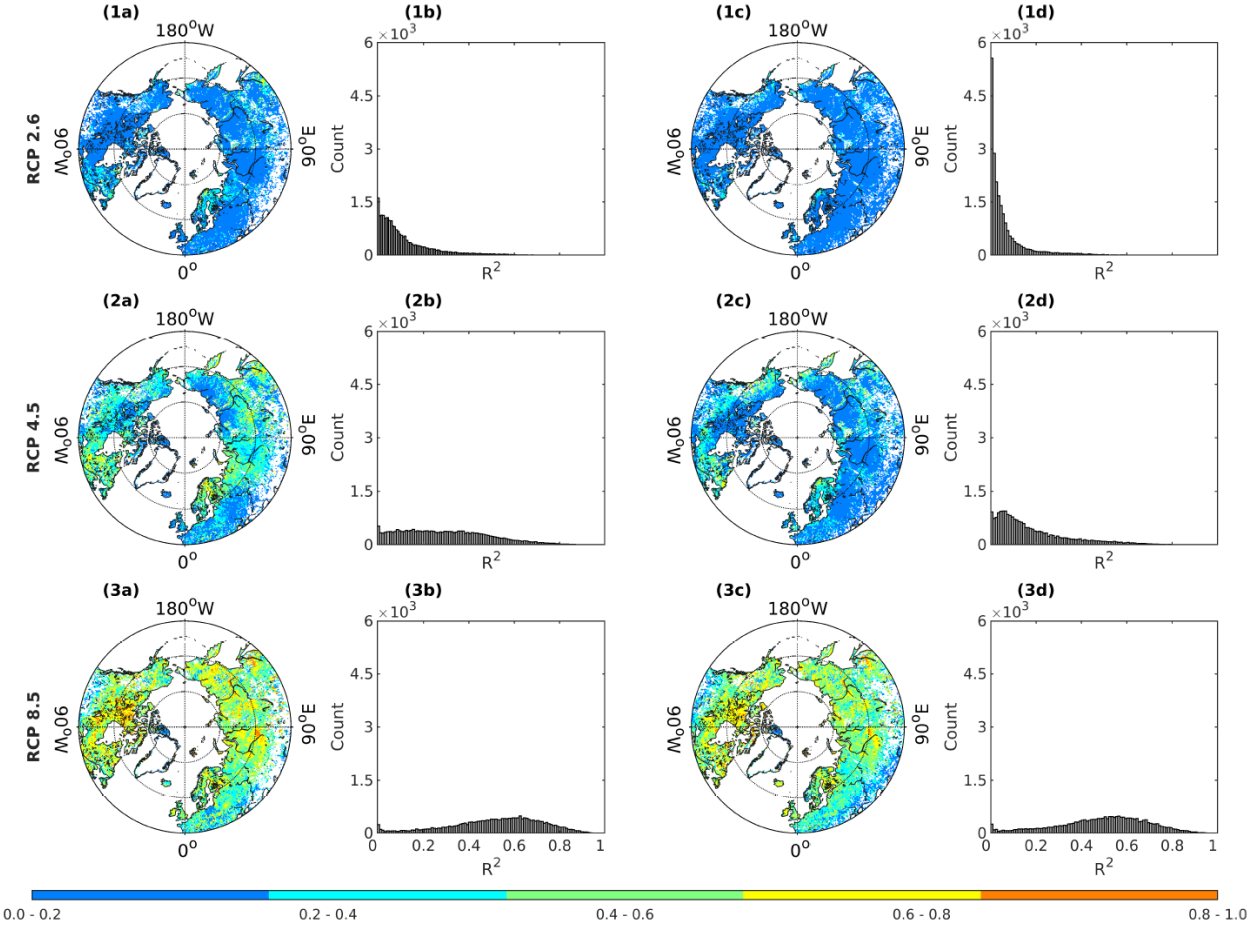

Figure S19. R^2 values and their histograms of the annual threshold temperature (°C) of peatland C sink-source shift. Panel (a): the R^2 values with IPSL-CM5A-LR forcing; panel (b): the histogram of panel (a); panel (c): the R^2 values with bcc-csm1-1 forcing; panel (d): the histogram of panel (c).

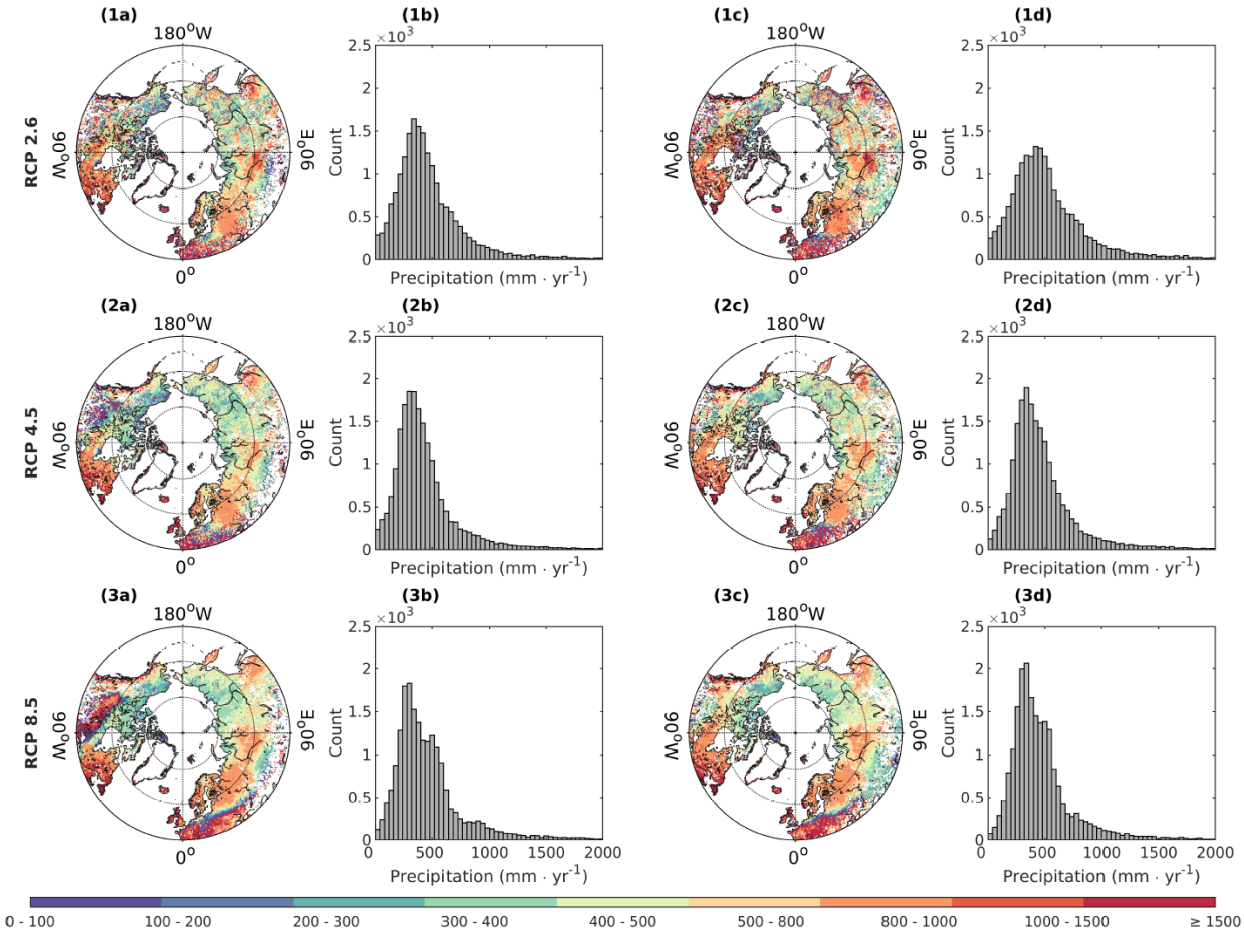

Figure S20. Threshold annual precipitation (mm) of peatland C sink-source shift. Panel (a): the threshold precipitation of IPSL-CM5A-LR forcing; panel (b): the histogram of panel (a); panel (c): the threshold precipitation of bcc-csm1-1 forcing; panel (d): the histogram of panel (c).

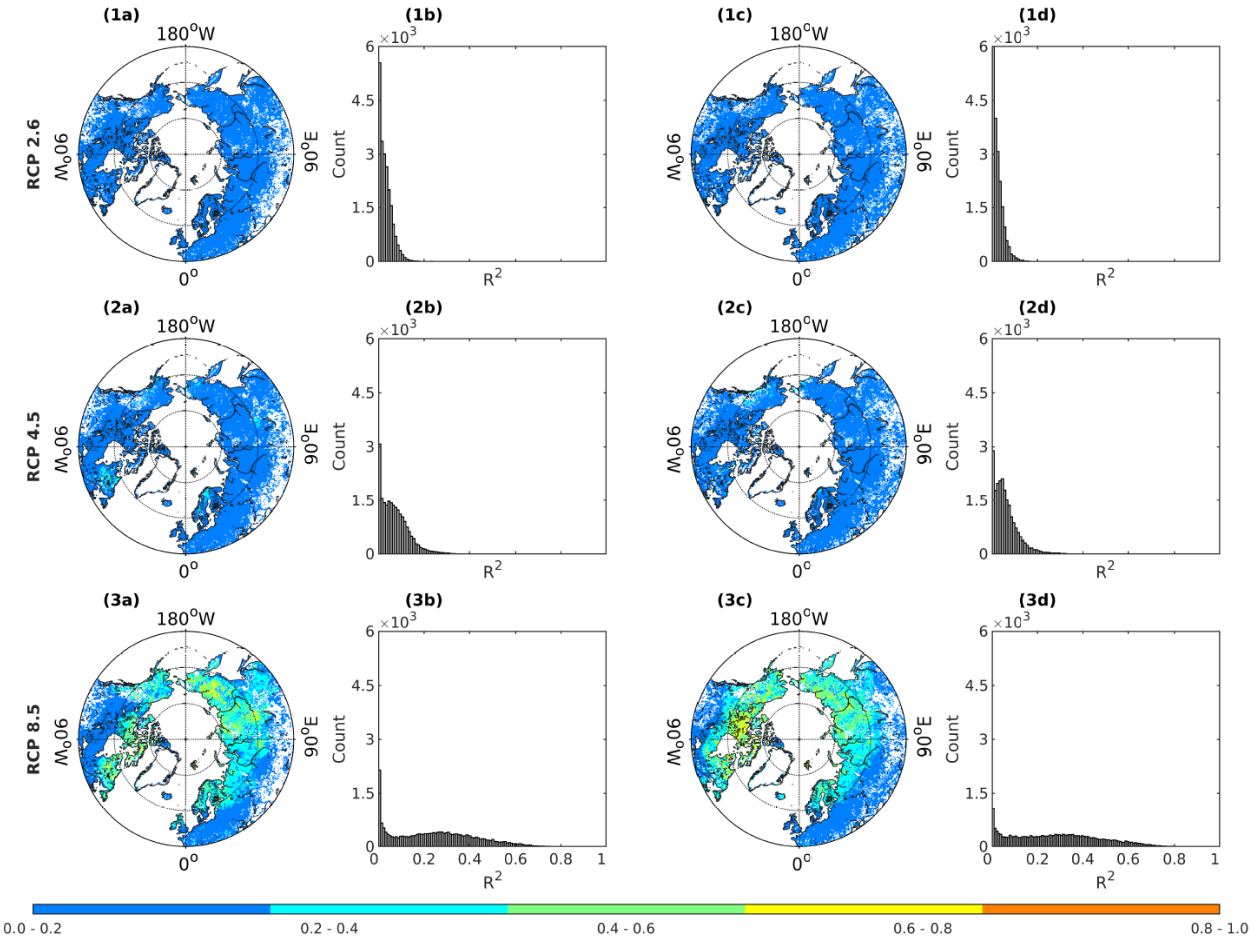

Figure S21. R^2 values and their histograms of the annual threshold precipitation (mm) of peatland C sink-source shift. Panel (a): the R^2 values with IPSL-CM5A-LR forcing; panel (b): the histogram of panel (a); panel (c): the R^2 values with bcc-csm1-1 forcing; panel (d): the histogram of panel (c).

Table S1. Comparison of initialization conditions under different forcing data and warming scenarios

CMIP5 forcing	Warming scenario	Potential peatland bin number (n)	Initial pan-Arctic peatland C storage in 1940 (Pg C)
IPSL-CM5A-LR	RCP 2.6	204549	333.2
	RCP 4.5	199343	330.7
	RCP 8.5	195910	328.7
bcc-csm1-1	RCP 2.6	208157	338.7
	RCP 4.5	203844	336.9
	RCP 8.5	198869	334.6

* Grid cells with less than 1% peatland coverage are not included.

Table S2. Annual temperature, precipitation, and the area of wetland, peatland and permafrost in 1990, 2100 and 2300

		IPSL-CM5A-LR			bcc-csm1-1		
		RCP 2.6	RCP 4.5	RCP 8.5	RCP 2.6	RCP 4.5	RCP 8.5
Temperature (°C)	1990	-4.1			-3.8		
	2100	-1.8	0.1	4.3	-1.8	-0.6	3.4
	2300	-2.6	1.4	12.5	-2.9	-0.2	10.3
Precipitation ($mm \cdot yr^{-1}$)	1990	463.3			459.8		
	2100	504.0	523.0	569.4	497.9	513.7	560.7
	2300	492.0	552.1	701.1	492.1	522.2	657.8
Wetland area (million km^2)	1990	2.6	2.5	2.5	2.6	2.6	2.6
	2100	2.0	1.6	1.1	2.2	2.0	1.4
	2300	2.1	1.4	0.2	2.3	1.8	0.5
Northern peatlands permafrost area (million km^2)	1990	2.1	2.1	2.0	2.0	1.9	1.9
	2100	1.9	1.4	0.8	1.8	1.7	0.9
	2300	2.0	1.5	0.3	1.9	1.6	0.3
Old peatland area (million km^2)	1990	2.5	2.5	2.5	2.6	2.5	2.5
	2100	2.5	2.5	2.5	2.6	2.5	2.5
	2300	2.5	2.5	2.1	2.6	2.5	2.4
New peatland area (million km^2)	1990	0.0	0.0	0.0	0.0	0.0	0.0
	2100	0.1	0.1	0.0	0.1	0.1	0.1
	2300	0.2	0.1	0.0	0.2	0.2	0.1
Total peatland area (million km^2)	1990	2.5	2.5	2.5	2.6	2.5	2.5
	2100	2.6	2.6	2.5	2.7	2.6	2.6
	2300	2.7	2.6	2.2	2.8	2.7	2.4

* Peatland refers to the region with peat thickness >= 30cm.

Table S3. Pan-Arctic total C stock and annual C fluxes in 1990, 2100 and 2300

		IPSL-CM5A-LR			bcc-csm1-1		
		RCP 2.6	RCP 4.5	RCP 8.5	RCP 2.6	RCP 4.5	RCP 8.5
C stock (Pg C)	1990	338.1	335.4	333.3	343.7	341.8	339.3
	2100	336.8	330.2	320.0	344.5	340.6	331.5
	2300	330.9	307.7	201.7	343.8	328.0	243.9
NPP ($TgC \cdot yr^{-1}$)	1990	362.2	355.0	352.4	377.6	373.1	366.2
	2100	361.4	348.2	350.9	390.7	391.5	387.7
	2300	354.4	340.0	297.5	381.4	413.2	339.0
CO_2 emission ($TgC \cdot yr^{-1}$)	1990	257.9	254.3	252.5	272.2	269.2	265.8
	2100	357.0	430.1	618.5	352.7	389.9	558.0
	2300	320.0	413.5	676.1	321.1	359.5	636.5
CH_4 emission ($TgC \cdot yr^{-1}$)	1990	31.8	31.7	31.7	33.8	33.7	33.7
	2100	42.4	59.2	118.8	42.3	49.5	92.9
	2300	37.9	62.9	210.7	37.9	48.5	140.5

* C stock includes both soil and vegetation C.

Table S4. Pan-Arctic peatlands C accumulation rate during four time periods

		IPSL-CM5A-LR			bcc-csm1-1		
		RCP 2.6	RCP 4.5	RCP 8.5	RCP 2.6	RCP 4.5	RCP 8.5
C accumulation rate ($gC \cdot m^{-2} \cdot yr^{-1}$)	1940-1990	32.5	31.9	31.8	32.1	32.1	31.5
	1990-2090	-3.0	-13.0	-33.5	3.0	-2.5	-18.5
	2090-2190	-12.3	-38.7	-169.0	-1.1	-18.2	-122.2
	2190-2290	-7.6	-36.9	-227.3	-1.9	-23.1	-163.8

* C accumulation rate is averaged from all grid cells weighted by the spatially-explicit peatland area.

Table S5. R^2 values of PTEM simulated pan-Arctic active layer depth (m) with ESACCI dataset

Forcing	1997	1998	1999	2000	2001	2002	2003	2004	2005	2006	2007
IPSL-CM5A-LR	0.54	0.52	0.54	0.48	0.56	0.55	0.58	0.55	0.58	0.6	0.5
bcc-csm1-1	0.48	0.44	0.52	0.54	0.51	0.45	0.6	0.46	0.54	0.53	0.52
	2008	2009	2010	2011	2012	2013	2014	2015	2016	2017	2018
IPSL-CM5A-LR	0.51	0.51	0.42	0.48	0.6	0.54	0.53	0.51	0.56	0.48	0.53
bcc-csm1-1	0.56	0.47	0.48	0.45	0.51	0.51	0.54	0.49	0.57	0.47	0.52

* R values are all positive.

* ESACCI is Essential Climate Variable Permafrost Climate Change Initiative (Obu et al., 2020).

Table S6. R^2 values of PTEM simulated Alaska active layer depth (m) with ABoVE dataset

Forcing	2001	2002	2003	2004	2005	2006	2007	2008
IPSL-CM5A-LR	0.25	0.27	0.28	0.39	0.32	0.28	0.27	0.33
bcc-csm1-1	0.26	0.37	0.26	0.33	0.35	0.23	0.28	0.29
	2009	2010	2011	2012	2013	2014	2015	
IPSL-CM5A-LR	0.26	0.31	0.18	0.22	0.30	0.25	0.36	
bcc-csm1-1	0.33	0.31	0.21	0.32	0.36	0.28	0.26	

* R values are all positive.

* ABoVE is Arctic-Boreal Vulnerability Experiment, the dataset is obtained from the subtopic of Active Layer Thickness from Remote Sensing Permafrost Model, Alaska, 2001-2015 (Yi and Kimball, 2020).

References

Hugelius, G., Loisel, J., Chadburn, S., Jackson, R. B., Jones, M., MacDonald, G., Marushchak, M., Olefeldt, D., Packalen, M., Siewert, M. B., Treat, C., Turetsky, M., Voigt, C., and Yu, Z.: Large stocks of peatland carbon and nitrogen are vulnerable to permafrost thaw, Proceedings of the National Academy of Sciences, 117, 20438, 10.1073/pnas.1916387117, 2020.

Melton, J. R., Chan, E., Millard, K., Fortier, M., Winton, R. S., Martín-López, J. M., Cadillo-Quiroz, H., Kidd, D., and Verchot, L. V.: A map of global peatland extent created using machine learning (Peat-ML), Geosci. Model Dev. Discuss., 2022, 1-44, 10.5194/gmd-2021-426, 2022.

Obu, J., Westermann, S., Barboux, C., Bartsch, A., Delaloye, R., Grosse, G., Heim, B., Hugelius, G., Irrgang, A., Kääb, A. M., Kroisleitner, C., Matthes, H., Nitze, I., Pellet, C., Seifert, F. M., Strozzi, T., Wegmüller, U., Wieczorek, M., and Wiesmann, A.: ESA Permafrost Climate Change Initiative (Permafrost_cci): Permafrost Climate Research Data Package v1., Centre for Environmental Data Analysis [dataset], https://catalogue.ceda.ac.uk/uuid/1f88068e86304b0fbd34456115b6606f, 2020.

Xu, J., Morris, P. J., Liu, J., and Holden, J.: PEATMAP: Refining estimates of global peatland distribution based on a meta-analysis, CATENA, 160, 134-140, https://doi.org/10.1016/j.catena.2017.09.010, 2018.

Yi, Y. and Kimball, J. S.: ABoVE: Active Layer Thickness from Remote Sensing Permafrost Model, Alaska, 2001-2015, 10.3334/ORNLDAAC/1760, 2020.

Zhao, B., Zhuang, Q., and Frolking, S.: Modeling carbon accumulation and greenhouse gas emissions of northern peatlands since the Holocene (in review), 2022.

Zomer, R. J. and Trabucco, A.: Version 3 of the "Global Aridity Index and Potential Evapotranspiration (ET0) Database": Estimation of Penman-Monteith Reference Evapotranspiration. (In Press). [dataset], https://cgiarcsi.community/2019/01/24/globalaridity-index-and-potential-evapotranspiration-climate-database-v3/, 2022.